

Process Planning of the Automatic Polishing of the Curved Surface Using a Five-axis Machining Tool

Lei Zhang

Soochow University

Chen Ding

Soochow University

Cheng Fan (✉ chfan@suda.edu.cn)

Suzhou University

Qian Wang

Soochow University

Kejun Wang

Soochow University

Original Article

Keywords: Curved surface, Path planning, Kinematics analysis, Polishing process

Posted Date: October 29th, 2021

DOI: <https://doi.org/10.21203/rs.3.rs-45971/v2>

License:  This work is licensed under a Creative Commons Attribution 4.0 International License.

[Read Full License](#)

Process planning of the automatic polishing of the curved surface using a five-axis machining tool

Lei Zhang¹, Chen Ding¹, Cheng Fan^{1*}, Qian Wang¹, Kejun Wang¹

1 Jiangsu Provincial Key Laboratory of Advanced Robotics , College of Mechanical and Electrical Engineering, Soochow University, Suzhou 215021, China

*Contact: Prof. Cheng Fan.

E-mail: chfan@suda.edu.cn

Process planning of the automatic polishing of the curved surface using a five-axis machining tool

Abstract Curved surface parts are widely used in aerospace industry, automotive industry and other fields due to their excellent features in aerodynamics, fluid dynamics and thermodynamics. Compared with the modeling technology of the curved surface, the development of the processing technology of the curved surface is slightly behind. In order to improve the processing quality and efficiency of the curved surface, this paper independently developed a five-axis CNC polishing machine tool, and studied the pre-processing and the post-processing when machining the curved surface. Taking a metal shell of the mobile phone as an example, three different paths are planned for the flat surface and the curved surface respectively, and a method for generating the tool path is proposed. The kinematics model of the five-axis CNC machine tool is established, which is used to obtain the calculation formula of the movement amount of each axis when polishing in the flat surface and the curved surface of the metal shell. The polishing effects of the different paths about the surface quality and the polishing efficiency of the metal shell are studied through the polishing experiments, and the polishing path with the best surface quality and the highest polishing efficiency is found.

Keywords: Curved surface, Path planning, Kinematics analysis, Polishing process

1 Introduction

The rapid development of the modern industry and its applications have put forward higher requirements on the appearance and performance of products. The products with curved surfaces are exquisite in appearance, controllable in geometry and flexible in shape. Having been widely used in products of all walks of life, they also have excellent features in aerodynamics, fluid dynamics and thermodynamics [1,2]. After decades of development, the modeling technology of the curved surface has

been relatively mature. However, because of its high requirements in precision and the difficulty in mathematical expressions, the curved surface machining has always been a major problem in the world today [3,4]. Polishing is essential for the traditional bathroom parts, shell parts in 3C industry and household kitchenware, and the key components in new industry such as blades, artificial bones, optical curved surfaces also require a final polishing process. As the last step in manufacturing process, the polishing process plays a vital role in the overall quality of the parts [5]. The traditional machining process of the curved surface adopts the ordinary machine tools or three-axis CNC machine tools, and then the final surface quality mainly relies on manual polishing. The surface quality after manual polishing is poor and the polishing efficiency is low. In recent years, the performance of the CNC machine tools has been improved greatly, especially the five-axis CNC machine tool, which integrates some advanced technologies such as computer control, high-performance servo drive and precision machining. Two rotation axes are added on the basis of the three-axis machine tools, which can avoid machining interference and improve the quality of the curved surface machining. After a work piece is clamped, multi-face machining can be achieved, which improves the machining efficiency and the machining accuracy[6-8].

The path planning in the polishing process has a direct impact on the polishing efficiency, quality and accuracy, and is one of the most important research contents in the polishing process. The path planning is the process of planning the polishing path of the machine tool according to the shell model after forming. A reasonable polishing path can improve the machining efficiency and reduce the costs. The polishing path should meet the conditions of no interference, continuous smoothness and high code quality [9,10]. The common methods of generating the tool path are

isoparametric method [11,12], isometric section plane method [13,14], equal residual height method [15,16], etc. Sun[17] et al. proposed a method based on a polyhedron model with triangular mesh for generating the tool path, which can naturally form a machining path along polyhedron model, and can reduce the tool wear and machining time. Gershon[18] et al. proposed a simple and practical isoparametric tool path for free-form surface. Can[19] et al. proposed a new method based on the equal residual height method for generating the tool path and optimized the path, so that the overall length of the tool path was reduced and the machining efficiency was significantly improved. Senatore[20] et al. proposed a simplified method for calculating the interference judgment of isometric lines, which greatly improved the calculation efficiency. Ding[21] et al. proposed an adaptive equal-plane method and applied iso-illuminance method to divide the surface area. For different areas, they applied different plane spacing to intersect the curved surface, and adopted different tool path planning to improve the surface quality. The technology of generating the tool path is one of the important contents of the CNC machining technology. The choice of the method for generating the tool path should be determined by combining the nature of the workpiece to be processed, the type of CNC machine tool, the machining process, the tool used and the CNC system, so as to realize the high quality and high efficiency machining process according to the generated path. However, many researchers only studied the polishing path, and there is no systematic study on the pre-processing and the post-processing for the five-axis machining tool. On this basis, the innovation of this paper is that this paper combined the polishing path planning, generation of tool location, kinematic analysis and generation of NC code, and systematically studied the polishing

technology of the five-axis machine tool. The research process of this paper is shown in Figure 1.

This paper is organized as follows. In section 2, the specific structure of the machine tool and the polishing tool system is introduced. Taking a mobile phone with a metal shell as an example, the path of the cutter contact point was determined, and then the path of the cutter location point was obtained by calculation in the polishing process. In section 3, a mathematical model of the five-axis CNC machine tool is established; the kinematic analysis is carried out and the formula for solving the movement amount of each axis is derived. In section 4, a five-axis CNC machine tool is used to carry out the polishing experiment on the metal shell of the mobile phone. The experiment verified the rationality of the different polishing paths and measured the surface roughness of the sample after polishing. By analyzing the experimental results, the path with the best polishing effect and the highest polishing efficiency was found.

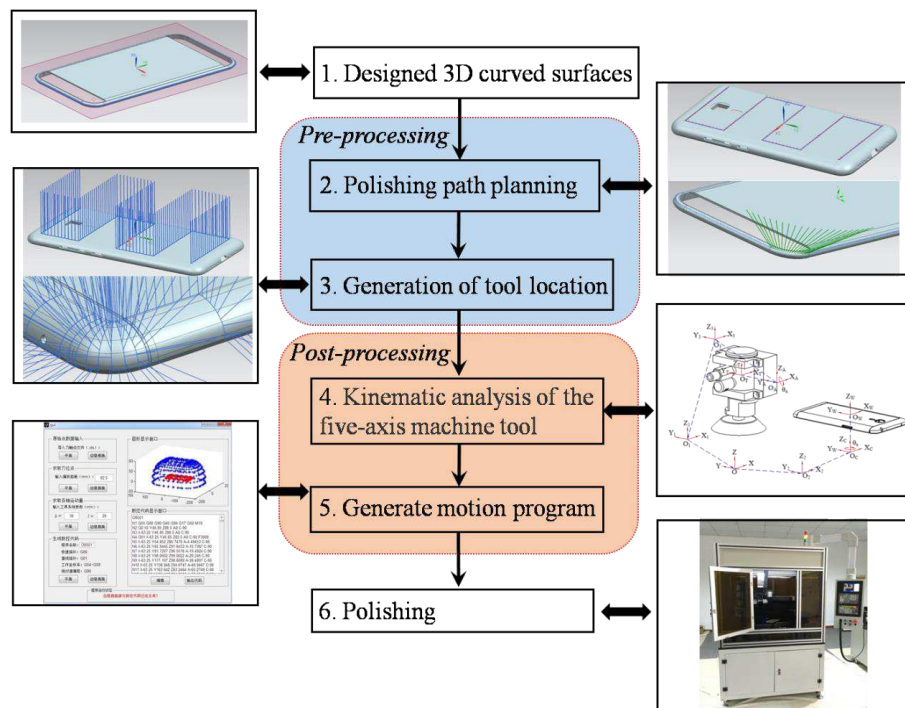


Figure 1 Process planning for polishing the curved surface

2 The five-axis CNC machine tool and the generation of the polishing path

2.1 The five-axis CNC machine tool

In this paper, a metal shell of the mobile phone is taken as an example to plan the polishing path, as is shown in Figure 2. The metal shell is mainly divided into three parts: the flat surface, the curved surface of edge and the high-gloss chamfered surface. Because the high-gloss chamfered surface is directly cut by the high-speed diamond cutter, it does not involve the polishing process. Thus, this paper only studies the generation of the polishing path of the flat surface and the curved surface. The overall size of the metal shell of the mobile phone is 150 mm×74.5 mm×7.6 mm, and the origin of the coordinate is established on the center of the flat surface.

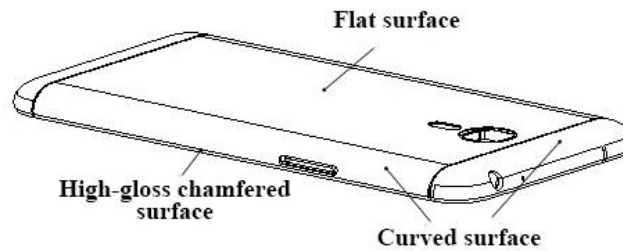
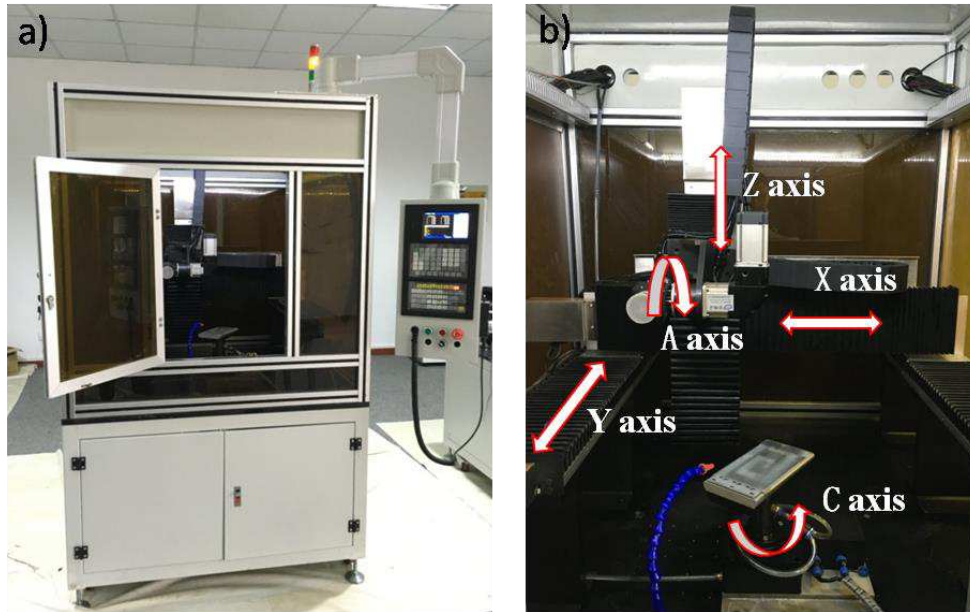


Figure 2 The model of the metal shell of the mobile phone

According to the structural characteristics of the curved-surface products, a polishing CNC machine tool with five axes is developed as shown in Figure 3.

The five axes of the machine tool refer to the X axis, Y axis, Z axis, A axis and C axis, wherein the X axis, Y axis and Z axis are three linear axes, and the A axis and C axis are two rotation axes. The coordinate system of the machine tool is established according to the polishing system of the metal shell. Z axis is perpendicular to the clamped surface of the workpiece, setting right as the positive direction of X axis when viewing from the polishing system to the column. Y axis is determined by right-hand

Cartesian coordinate system after the positive direction of X axis and Z axis are determined. The positive directions of the A axis and C axis are determined according to the right-hand screw rule.



(a)The appearance of the machine tool (b) The internal structure of the machine tool

Figure 3 The polishing CNC machine tool with five axes

Figure 4 shows the model of the polishing tool system. The polishing tool system is mainly composed of a connecting plate of Z axis, a drive motor, a turbine reducer, a pneumatic locking device and a pneumatic rotation tool. Among them, the pneumatic rotation tool is mainly composed of the ventilation part, the sandpaper plate and the sponge sandpaper. Sponge sandpaper can be directly adhered to the sandpaper plate of the pneumatic rotation tool, which is driven by the pneumatic rotation tool at high speed. The pneumatic rotation tool can be fixed in a certain posture to polish the flat surface, or it can be driven by the drive motor to rotate around the A axis to polishing the curved surface of the edge.

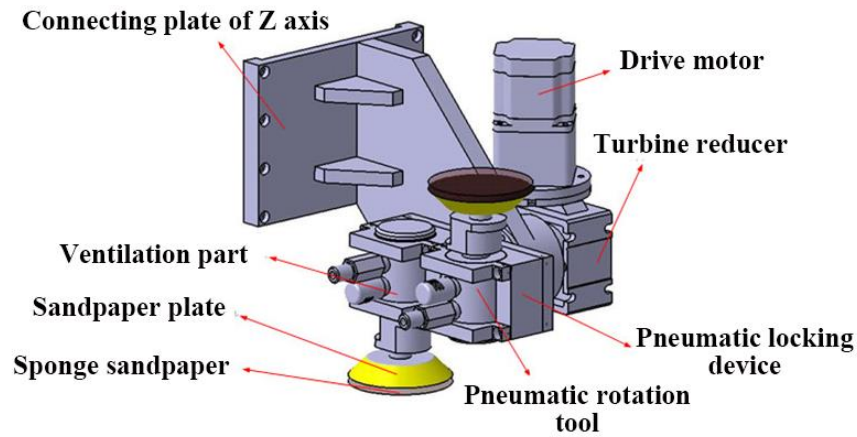


Figure 4 The polishing tool system

2.2 Pre-processing for the polishing process

2.1.1 The path generation of the cutter location point of the flat surface

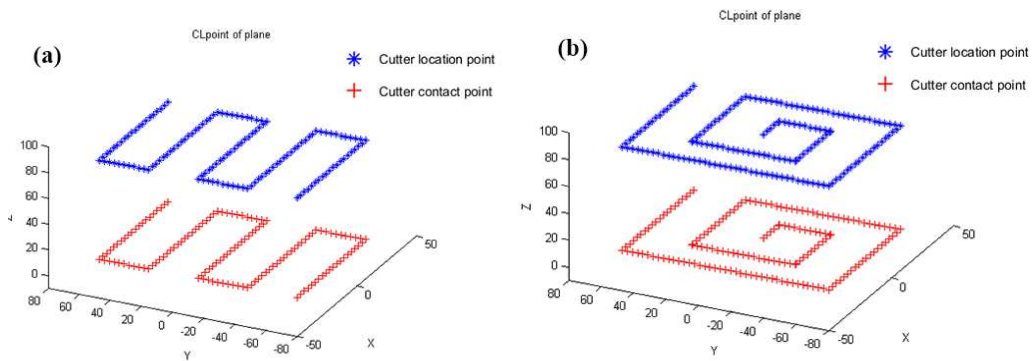
The size of the flat surface of the metal shell is 132mm × 60mm, and the diameter of the sponge sandpaper is 75mm. The data of the cutter contact point includes two parts: point data and normal vector data. The path of the cutter contact point of the flat surface is obtained by the model of the metal shell. When polishing the flat surface, the polishing ways include the lateral polishing, longitudinal polishing and diagonal polishing. In this section, three different polishing paths are planned according to the size of the flat surface and the diameter of the sponge sandpaper: "unilateral isoparametric path", "spiral isoparametric path" and "oblique cross path".

Let the thickness of the sponge sandpaper be h . The vertical distance between the working surface of the sandpaper plate and the A axis is R . The cutter location point can be obtained by offsetting the cutter contact point in the direction of the normal vector. The offset distance is the sum of the thickness of the sponge sandpaper and the vertical distance between the working surface of the sandpaper plate and the A axis, which is $R+h$. Let the coordinate of the cutter contact point be (x_i, y_i, z_i) . Let the normal vector of

the flat surface be $(0, 0, 1)$. Then the calculation formula of the coordinate of the cutter location point (x_j, y_j, z_j) is

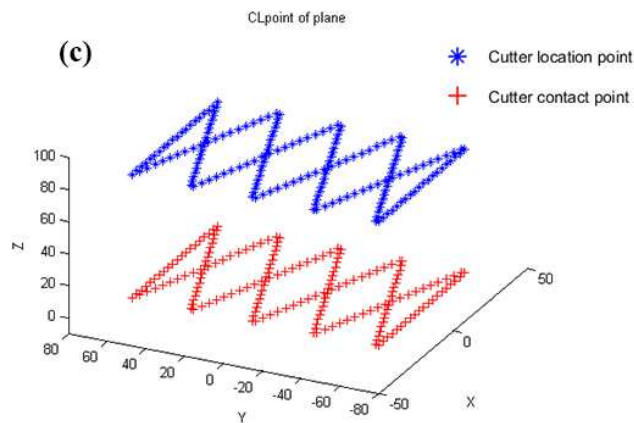
$$\begin{cases} x_j = x_i \\ y_j = y_i \\ z_j = z_i + R + h \end{cases} \quad (1)$$

As shown in Figure 5, by importing the coordinate value of the cutter location point in MATLAB, three different paths of the cutter location point can be obtained respectively.



(a) Unilateral isoparametric path

(b) Spiral isoparametric path



(c) Oblique cross path

Figure 5 The paths of the cutter location point of the flat surface

2.1.2 The path generation of the cutter location points of the curved surface

When polishing the curved surface, the polishing ways include the annular polishing, lateral polishing and oblique polishing. According to the modeling characteristics of the curved surface, three different polishing paths of the cutter contact points are planned: “annular path”, “L-shaped path” and “V-shaped path”.

Figure 6 shows the schematic diagram for calculating the path of the cutter location point of the curved surface. Let the thickness of the sponge sandpaper be h . The vertical distance between the working surface of the sandpaper plate and the A axis is R . The cutter location point can be obtained by offsetting the cutter contact point in the direction of the normal vector. The offset distance is the sum of the thickness of the sponge sandpaper and the vertical distance between the working surface of the sandpaper plate and the A axis, which is $R+h$. Let the coordinate of the cutter contact point be $M(x_i, y_i, z_i)$. Let the unit normal vector be $P(l_i, m_i, n_i)$. Then the calculation formula of the coordinate of the cutter location point $N(x_j, y_j, z_j)$ is

$$\begin{cases} x_j = x_i + l_i \cdot (R + h) \\ y_j = y_i + m_i \cdot (R + h) \\ z_j = z_i + n_i \cdot (R + h) \end{cases} \quad (2)$$

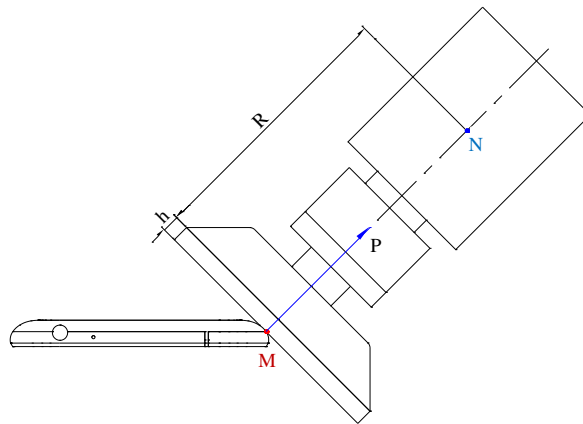


Figure 6 The schematic diagram for calculating the path of the cutter location point of the curved surface

As shown in Figure 7, by importing the coordinate value of the cutter location point in MATLAB, three different paths of the cutter location point can be obtained respectively.

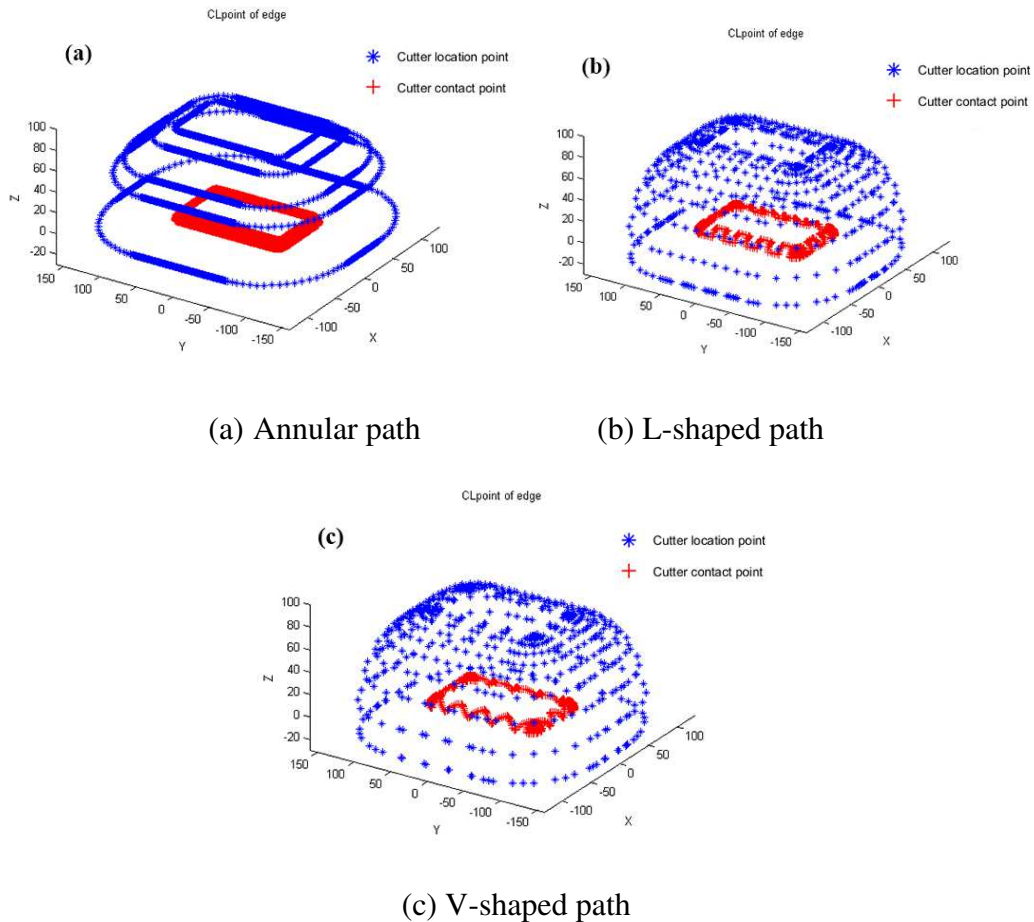


Figure 7 The paths of the cutter location point of the curved surface

3 Post-processing for the five-axis machining tool

The model of the workpiece can be used to generate the path of the cutter contact point and the normal vector of the cutter shaft, so as to obtain the path of the cutter location, which is pre-processing in the polishing process. However, the data file of the cutter location point generated by the pre-processing cannot be directly recognized and executed by the CNC system. Therefore, it is necessary to obtain the movement amount of each axis in the polishing process through kinematic analysis according to the specific structure of the machine tool, and then convert the movement data of each axis

into the NC code file that can be executed by the control system of the machine tool. The above process of converting the cutter location data file to NC code file is post-processing.

3.1 The kinematics model of the five-axis CNC machine tool

According to the structure of the five-axis CNC machine tool, the kinematic model of the machine tool is established as shown in Figure 8. The workpiece coordinate system is expressed as $O_W X_W Y_W Z_W$, and the origin of the coordinate is established at the center of the flat surface of the metal shell. The coordinate system of C axis is expressed as $O_C X_C Y_C Z_C$, and the origin of the coordinate is established at the rotation center of the C-axis turntable. The Z_C axis and the Z_W axis are on the same straight line. The coordinate system of Y axis is expressed as $O_2 X_2 Y_2 Z_2$, and the origin of the coordinate is established at the center of the saddle surface of the Y-axis electric actuator. The coordinate system of the machine tool is expressed as OXYZ, and the origin of the coordinate is established at the zero point of the machine tool. The coordinate system of X axis is expressed as $O_1 X_1 Y_1 Z_1$, and the origin of the coordinate is established at the center of the saddle surface of the X-axis electric actuator. The coordinate system of Z axis is expressed as $O_3 X_3 Y_3 Z_3$, and the origin of the coordinate is established at the center of the saddle surface of the Z-axis electric actuator. The coordinate system of A axis is expressed as $O_A X_A Y_A Z_A$, and the origin of the coordinate is established at the rotation center of the A axis. The coordinate system of the tool is expressed as $O_T X_T Y_T Z_T$, and the origin of the coordinate is established at the rotation center of the pneumatic rotation tool. The Y_T axis and the Y_A axis are on the same straight line. The coordinate of the origin of the tool coordinate system in the A-axis coordinate system is $(0, b, 0)$.

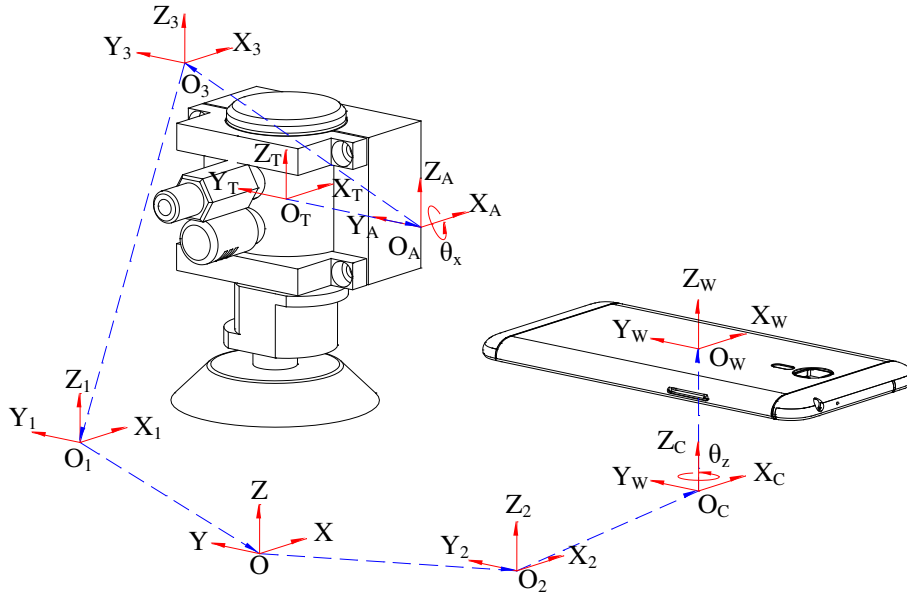


Figure 8 The kinematics model of the five-axis CNC machine tool

3.2 Inverse kinematics of the five-axis machine tool

The solution of the inverse kinematics is a process of solving the movement amount of each axis of the machine tool according to the data of the cutter location point generated by pre-processing, also known as kinematics analysis. The movement amount of each axis includes the movement amount along X axis, the movement amount along Y axis, the movement amount along Z axis, the rotation amount of A axis and the rotation amount of C axis, which are respectively expressed by dx , dy , dz , θ_x and θ_z . When solving the movement amount of each axis, according to the principle that the workpiece is relative rest and the tool is relative motion, the origin of the cutter coordinate system is transformed to the workpiece coordinate system through coordinate transformation and coincides with the cutter location point. Through the rotation of two rotation axes, the normal vector of the cutter shaft is ensured to be parallel to the normal vector of each cutter location point.

3.2.1 Solving the rotation angle around A axis and C axis

First of all, the rotation angles around A axis and C axis are calculated according to the normal vector of the cutter contact point. As is shown in Figure 9, the workpiece coordinate system is expressed as $O_w X_w Y_w Z_w$. The unit normal vector of the cutter shaft is $\mathbf{O}_w \mathbf{T} = (l_i, n_i, m_i)$. In order to make the normal vector of the cutter shaft parallel to the positive direction of the Z_w axis, first rotate the normal vector of the cutter shaft anticlockwise around the Z_w axis by angle θ_z to the plane $Y_w Z_w$, and then rotate it anticlockwise around the X_w axis by angle θ_x to Z_w axis.

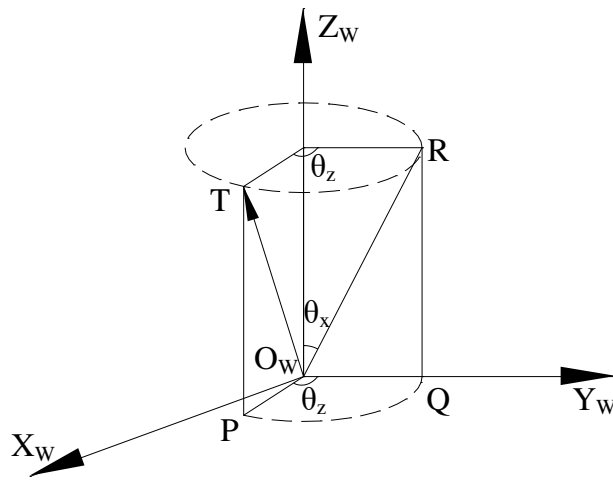


Figure 9 The rotation diagram of the normal vector of the cutter shaft

According to the geometrical relationship in Figure 10, the following formulas can be derived:

$$\begin{cases} \theta_x = \arctan(n_i / \sqrt{l_i^2 + m_i^2}) - \pi/2 \\ \theta_z = \arctan(m_i / l_i) - \pi/2 \end{cases} \quad (3)$$

3.2.2 Solving the movement amount along X axis, Y axis and Z axis

According to the inverse kinematics, the movement amounts of the machine tool along X axis, Y axis and Z axis are solved as follows.

The transformation matrix of the origin of the cutter coordinate system in the A-axis

coordinate system is

$$Trans(0,b,0) = \begin{bmatrix} 1 & 0 & 0 & 0 \\ 0 & 1 & 0 & b \\ 0 & 0 & 1 & 0 \\ 0 & 0 & 0 & 1 \end{bmatrix} \quad (4)$$

The transformation matrix rotating around the A axis is

$$Rot(x,\theta_x) = \begin{bmatrix} 1 & 0 & 0 & 0 \\ 0 & \cos \theta_x & -\sin \theta_x & 0 \\ 0 & \sin \theta_x & \cos \theta_x & 0 \\ 0 & 0 & 0 & 1 \end{bmatrix} \quad (5)$$

The transformation matrix of the origin of the A-axis coordinate system in the cutter coordinate system is

$$Trans(0,-b,0) = \begin{bmatrix} 1 & 0 & 0 & 0 \\ 0 & 1 & 0 & -b \\ 0 & 0 & 1 & 0 \\ 0 & 0 & 0 & 1 \end{bmatrix} \quad (6)$$

The transformation matrix of the cutter coordinate system moving along the X axis, Y axis, and Z axis in the workpiece coordinate system is

$$Trans(d_x,d_y,d_z) = \begin{bmatrix} 1 & 0 & 0 & d_x \\ 0 & 1 & 0 & d_y \\ 0 & 0 & 1 & d_z \\ 0 & 0 & 0 & 1 \end{bmatrix} \quad (7)$$

The transformation matrix rotating around the C axis is

$$Rot(z, \theta_z) = \begin{bmatrix} \cos \theta_z & -\sin \theta_z & 0 & 0 \\ \sin \theta_z & \cos \theta_z & 0 & 0 \\ 0 & 0 & 1 & 0 \\ 0 & 0 & 0 & 1 \end{bmatrix} \quad (8)$$

M_{WT} is used to represent the transformation matrix that coincides the origin of the cutter coordinate system with the cutter location point in the workpiece coordinate system.

$$M_{WT} = Rot(z, \theta_z) \cdot Trans(d_x, d_y, d_z) \cdot Trans(0, -b, 0) \cdot Rot(x, \theta_x) \cdot Trans(0, b, 0) \quad (9)$$

The coordinate of the cutter location point in the workpiece coordinate system is

$$p_w = [x_j \quad y_j \quad z_j \quad 1]^T \quad (j=1, 2, \dots, n) \quad (10)$$

The coordinate of the origin of the cutter coordinate system in the cutter coordinate system is

$$p_T = [0 \quad 0 \quad 0 \quad 1]^T \quad (11)$$

The origin of the cutter coordinate system is transformed to the workpiece coordinate system through coordinate transformation and coincides with the cutter location point, that is

$$p_w = M_{WT} \cdot p_T \quad (12)$$

By solving the Equation (12), the movement amount along X axis, Y axis and Z axis can be obtained.

$$\begin{cases} d_x = x_j \cdot \cos \theta_z + y_j \cdot \sin \theta_z \\ d_y = -x_j \cdot \sin \theta_z + y_j \cdot \cos \theta_z - b \cdot \cos \theta_x + b \\ d_z = z_j - b \cdot \sin \theta_x \end{cases} \quad (13)$$

Equation (3) and Equation (13) constitute the movement amount of each axis of the machine tool, that is

$$\begin{cases} d_x = x_j \cdot \cos \theta_z + y_j \cdot \sin \theta_z \\ d_y = -x_j \cdot \sin \theta_z + y_j \cdot \cos \theta_z - b \cdot \cos \theta_x + b \\ d_z = z_j - b \cdot \sin \theta_x \\ \theta_x = \arctan(n_i / \sqrt{l_i^2 + m_i^2}) - \pi/2 \\ \theta_z = \arctan(m_i / l_i) - \pi/2 \end{cases} \quad (14)$$

When polishing the flat surface of the metal shell, all the points in the flat surface are in the XOY plane, so the normal vectors of all the polished points in the flat surface are (0, 0, 1). By substituting it into Equation (14), the formula for calculating the movement amount of each axis when polishing in the flat surface can be obtained.

$$\begin{cases} d_x = -y_j \\ d_y = x_j \\ d_z = z_j \\ \theta_x = 0 \\ \theta_z = -\pi/2 \end{cases} \quad (15)$$

When polishing the curved surface of the metal shell, in order to prevent the collision between the pneumatic rotation tool and other mechanisms, the position of the pneumatic rotation tool needs to be adjusted in the YOZ plane, as is shown in Figure 10.

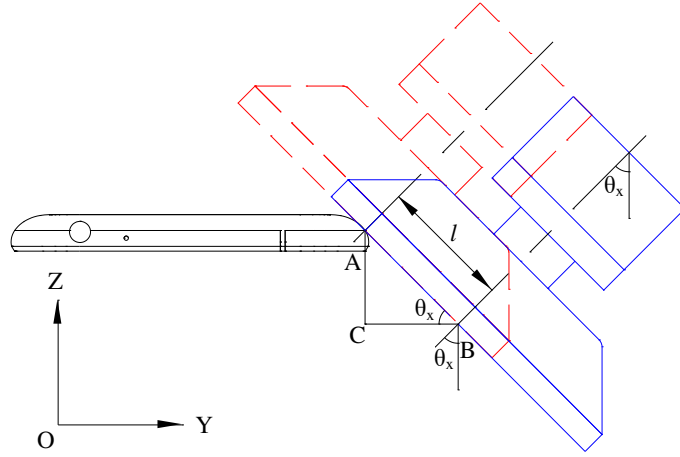


Figure 10 Adjusting the position of the tool

Move the axis of the pneumatic rotation tool from point A to point B along the tangent direction of the polished point. The distance between the point A and point B is l . The initial position of the axis of the pneumatic rotation tool is vertical. In the position shown in the Figure 10, the axis of the pneumatic rotation tool turns clockwise by an angle θ_x . In the process of moving the axis of the pneumatic rotation tool from point A to point B, the movement amount of Y axis increases by $l \cdot \cos(-\theta_x)$ and the movement amount of Z axis reduces by $l \cdot \sin(-\theta_x)$. By substituting the increasement of Y axis and the decrease of Z axis into the equation (14), we can get the calculation formula of the movement amount of each axis when polishing the curved surface of the metal shell, which gives

$$\begin{cases} d_x = x_j \cdot \cos \theta_z + y_j \cdot \sin \theta_z \\ d_y = -x_j \cdot \sin \theta_z + y_j \cdot \cos \theta_z - b \cdot \cos \theta_x + b + l \cdot \cos(-\theta_x) \\ d_z = z_j - b \cdot \sin \theta_x - l \cdot \sin(-\theta_x) \\ \theta_x = \arctan(n_i / \sqrt{l_i^2 + m_i^2}) - \pi/2 \\ \theta_z = \arctan(m_i / l_i) - \pi/2 \end{cases} \quad (16)$$

In conclusion, the calculation formulations of the inverse kinematics of the machine tool are shown in Table 1.

Table 1 The calculation formulations of inverse kinematics of the machine tool

Polishing position	Calculation formulations
Flat surface	$\begin{cases} d_x = -y_j \\ d_y = x_j \\ d_z = z_j \\ \theta_x = 0 \\ \theta_z = -\pi/2 \end{cases}$
Curved surface	$\begin{cases} d_x = x_j \cdot \cos \theta_z + y_j \cdot \sin \theta_z \\ d_y = -x_j \cdot \sin \theta_z + y_j \cdot \cos \theta_z - b \cdot \cos \theta_x + b + l \cdot \cos(-\theta_x) \\ d_z = z_j - b \cdot \sin \theta_x - l \cdot \sin(-\theta_x) \\ \theta_x = \arctan(n_i / \sqrt{l_i^2 + m_i^2}) - \pi/2 \\ \theta_z = \arctan(m_i / l_i) - \pi/2 \end{cases}$

4 Experiments

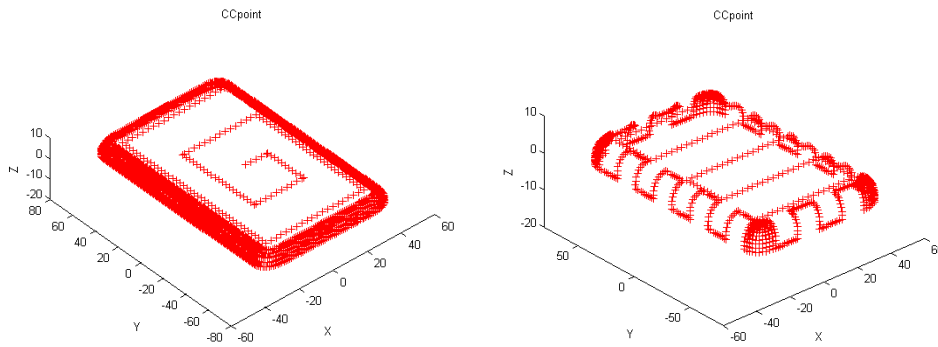
4.1 Planning of the experiments

According to the contents of the path planning in section 2, three different polishing paths are generated for the flat surface and the curved surface of the sample respectively. Then, by using the post-processing technology to convert the data file of the cutter location point into NC code file, the polishing experiment can be carried out by the five-axis CNC machine tool. The experiments are carried out in three groups, and the path forms of three groups are shown in Table 2.

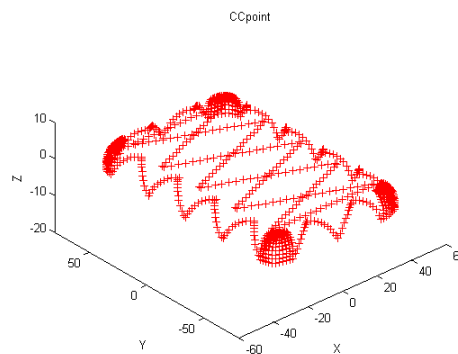
Table 2 The path forms of the polishing experiment

Number	Path forms of the curved surface	Path forms of the flat surface
1	Annular path	Spiral isoparametric path
2	L-shaped path	Unilateral isoparametric path
3	V-shaped path	Oblique cross path

In the process of the polishing experiment, the curved surface is first polished, and then the flat surface is polished. By using the drawing function of MATLAB, three paths of the cutter contact point are shown in Figure 11 (a), Figure 11 (b) and Figure 11 (c) respectively.



(a) The path of the cutter contact point in Experiment 1 (b) The path of the cutter contact point in Experiment 2



(c) The path of the cutter contact point in Experiment 3

Figure 11 The paths of the cutter contact points in three experiments

The abrasive of the sponge sandpaper is alumina, and the basal body is foamed PU sponge. The original thickness of the sponge sandpaper is 5mm. The sponge sandpaper with particle size of P800 is selected for coarse grinding and P1800 is selected for fine grinding.

4.2 Result and discussion

During the polishing experiment, the polishing state of the four typical positions of the metal shell are shown in Figure 12. The four typical positions of the metal shell are arc sphere of the curved surface, the short arc cylinder of the curved surface, the long arc cylinder of the curved surface and the flat surface.

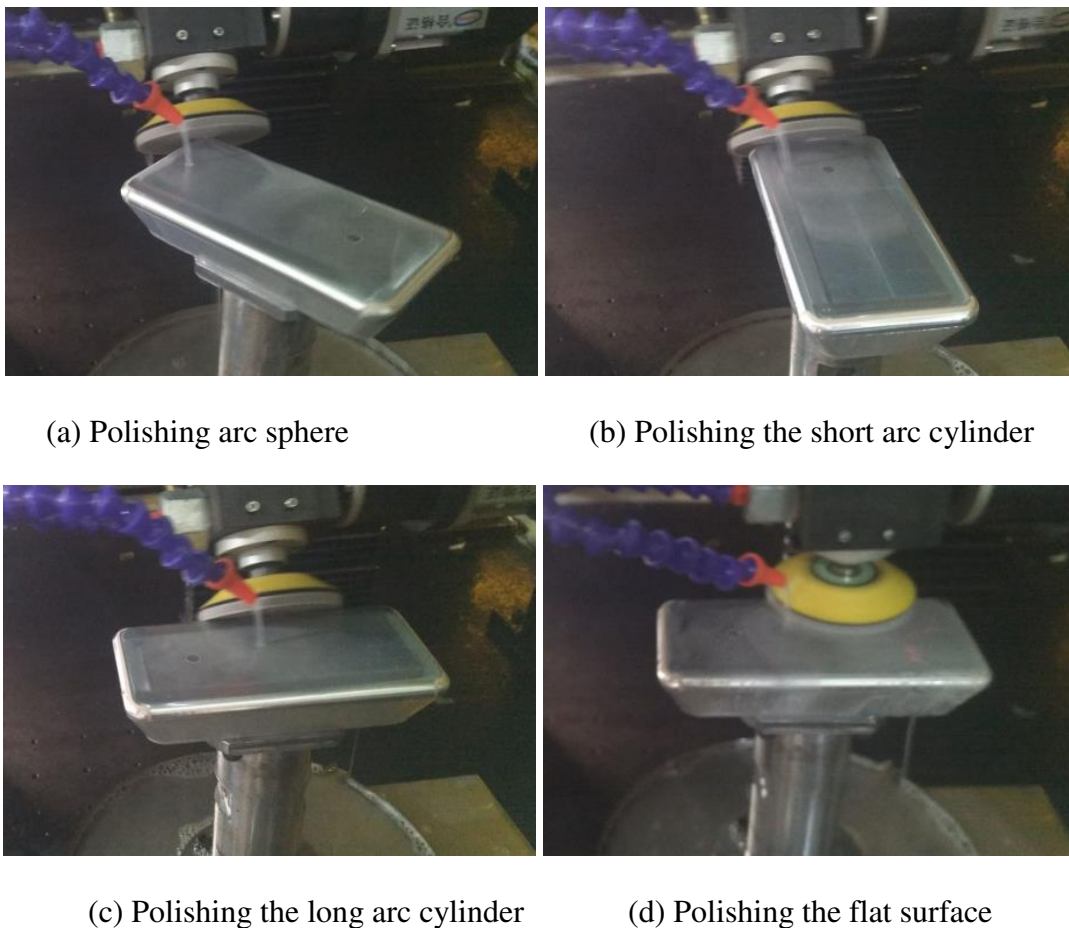


Figure 12 The polishing state of four typical positions

The polishing time of the flat surface and the curved surface were counted respectively in Experiment 1, Experiment 2 and Experiment 3 and the surface roughness of the flat surface and the curved surface were measured respectively in Experiment 1, Experiment 2 and Experiment 3. The sampling length is 0.8mm, and the evaluation length is 5 times of the sampling length. The digital filter is Gaussian filter. The experimental data is summarized in Table 3.

Table 3 The surface roughness and the polishing time of the polished sample

Experiment number	Surface roughness (Ra/ μm)		Polishing time (T/s)	
	Curved surface	Flat surface	Curved surface	Flat surface
1	0.2729	0.2392	42	9
2	0.2196	0.2106	112	7
3	0.1798	0.1608	104	12

The surface roughness of the curved surface of the unpolished sample is $0.7286\mu\text{m}$ and the surface roughness of the flat surface of the unpolished sample is $0.6968\mu\text{m}$. The surface roughness of the unpolished sample is large and the surface is uneven.

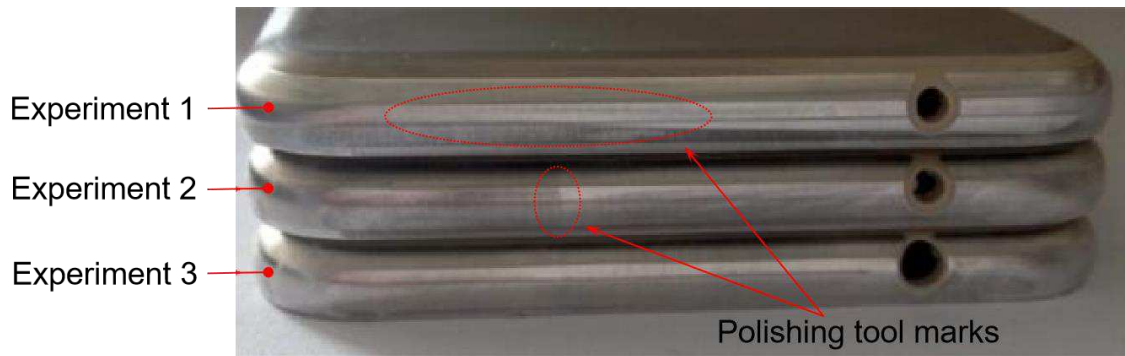


Figure13 Polishing effect of curved surface at the edge

As is shown in Table 3, the surface roughness of the curved surface in three experiments are $0.2972\mu\text{m}$, $0.2196\mu\text{m}$ and $0.1978\mu\text{m}$ respectively and the surface roughness of the flat surface are $0.2392\mu\text{m}$, $0.2106\mu\text{m}$ and $0.1608\mu\text{m}$ respectively. The profile of the surface roughness is more uniform compared with the unpolished sample

and the surface quality is improved. Among three experiments, the surface roughness in Experiment 3 is the smallest, and the polishing effect is the best. The surface roughness of the flat surface and the curved surface both meet the requirement. The polishing effect of the curved surface is shown in Figure 13. From top to bottom are the polishing effects of the curved surface of Experiment 1, Experiment 2 and Experiment 3. The polishing effect of Experiment 1 and Experiment 2 was not uniform, and there were visible machining knife marks on the surface after polishing. Compared with Experiment 1 and Experiment 2, the polishing effect of Experiment 3 was more uniform, and the surface was smooth without obvious knife marks.

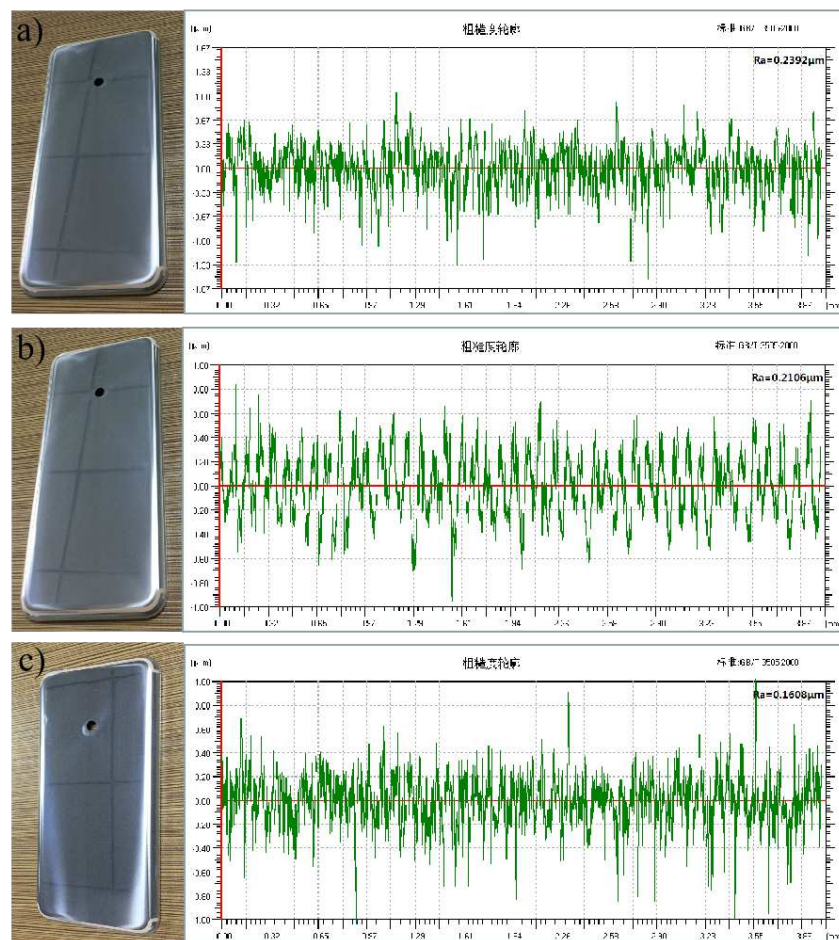


Figure 14 Polishing results: a) Polished roughness of Experiment 1 ($Ra=0.2393\mu\text{m}$), b) Polished roughness of Experiment 2 ($Ra=0.2106\mu\text{m}$) and c) Polished roughness of Experiment 3 ($Ra=0.1608\mu\text{m}$)

From the three experiments, the profiles of the surface roughness are shown in Figure 14. Compared with the unpolished samples, the roughness profile changes more evenly and the surface quality is improved. In Experiment 3, the surface roughness profile changes the least, and the polishing effect is the best.

By comparing the surface roughness of three experiments, it can be concluded that the surface roughness of the curved surface is larger than that of the flat surface. This is because when polishing the sample, the curved surface is first polished and then the flat surface is polished. The abrasive distributed on the sponge is sharper at the beginning of the polishing process. With the development of the polishing process, the sharp abrasive is gradually smoothed and the distribution of the abrasive is more uniform, so the above phenomenon appears.

Comparing the polishing time of three experiments, the polishing time of Experiment 1 is the shortest and the polishing efficiency is the highest when polishing the curved surface of the sample. When polishing the flat surface of the sample, the polishing time of Experiment 2 is the shortest and the polishing efficiency is the highest. However, the surface roughness of two parts of the sample in Experiment 1 and Experiment 2 does not meet the requirement after polishing.

From the above, considering the effects of surface roughness and the polishing efficiency, the polishing path of Experiment 3 is selected in the actual polishing process.

5 Conclusions

In this paper, a polishing CNC machine tool with five-axis was developed according to the characteristics of the curved surface. Taking a metal shell of the mobile phone as an example, three paths named "unilateral isoparametric path", "spiral isoparametric path"

and "oblique cross path" were planned for polishing the flat surface, and three paths named "annular path", "L-shaped path" and "V-shaped path" were planned for polishing the curved surface. Established the kinematics model of the five-axis CNC machine tool, and analyzed the kinematics model to obtain the calculation formula of the movement amount of each axis when polishing in the flat surface and the curved surface of the metal shell.

The polishing experiments were carried out by the five-axis CNC machine tool to polish the surface of the metal shell. The surface roughness of the curved surface in three experiments are $0.2972\mu\text{m}$, $0.2196\mu\text{m}$ and $0.1978\mu\text{m}$ respectively, and the surface roughness of the flat surface in three experiments are $0.2392\mu\text{m}$, $0.2106\mu\text{m}$ and $0.1608\mu\text{m}$ respectively. Among three experiments, the surface roughness in Experiment 3 is the smallest, and the polishing effect is the best. The surface roughness of the flat surface and the curved surface both meet the requirement. Comparing the polishing time of three experiments, the polishing time of Experiment 1 is the shortest and the polishing efficiency is the highest when polishing the curved surface of the sample. When polishing the flat surface of the sample, the polishing time of Experiment 2 is the shortest and the polishing efficiency is the highest. However, the surface roughness of two parts of the sample in Experiment 1 and Experiment 2 does not meet the requirement after polishing. From the above, considering the effects of surface roughness and the polishing efficiency, the polishing path of Experiment 3 is selected in the actual polishing process.

Availability of data and material: The datasets analyzed during the current study are available from the corresponding author on reasonable request.

Code availability: Not applicable

Author contribution: Investigation, Chen Ding and Cheng Fan; Project administration, Cheng Fan and Lei Zhang; Validation, Cheng Fan; Writing – original draft, Cheng Fan and Chen Ding; Writing – review & editing, Lei Zhang. All authors read and approved the final manuscript.

Funding

Supported by the National Natural Science Foundation of China [Grant No. 51975392], the Natural Science Foundation of the Jiangsu Higher Education Institutions of China [Grant No. 19KJA220001], the Postdoctoral Science Foundation of China [Grant No. 2015M571800] and the Natural Science Foundation of Jiangsu Province [Grant No. BK20201412].

Declarations

Ethics approval: Not applicable

Consent to participate: Not applicable

Consent for publication: Not applicable

Conflict of interest: The authors declare no competing interests.

References

1. Lee S, Yang S (2002) CNC tool-path planning for high-speed high-resolution machining using a new tool-path calculation algorithm. *Int J Adv Manuf Tech* 20(5): 326-333.

2. Chen T, Ye P Q (2002) A tool path generation strategy for sculptured surfaces machining. *J Mater Process Tech* 127(3): 369-373.
3. Xu K, Sasahara H (2016) “Generation of uniformly aligned dimples on a curved surface using a curved-surface, patch-division milling technique.” *International Journal of Automation Technology* 10(1): 23-29.
4. Ma W J, Wang F J, Jia Z Y (2016) “Machining parameter optimization in high-speed milling for inconel 718 curved surface.” *Mater Manuf Process* 31(13): 1692-1699.
5. Feng D Y, Sun YW, Du H P (2014) Investigations on the Automatic Precision Polishing of Curved Surfaces Using a Five-Axis Machining Centre. *Int J Adv Manuf Tech* 72: 1625—1637.
6. Fan J H, Ball A (2008) Quadric method for cutter orientation in five-axis sculptured surface machining. *Int J Mach Tool Manu* 48(7-8): 788-801.
7. Masuda T, Morishige K (2010) The Tool Path Generation by Using Configuration Space for Five-Axis Controlled Machining-Application to Rough Cutting by Using Square End Mill. *Key Engineering Materials* 447: 292-296.
8. Wang S C, Wang H J, Han Q S (2019) “Analysis of dynamic characteristics of five-axis CNC machine tool.” *The Journal of Engineering* 23: 8790-8793.
9. Chaves-Jacob J, Linares J M, Spraul J M (2015) Control of the contact force in a pre-polishing operation of free-form surfaces realised with a 5-axis CNC machine. *Cirp Ann-Manuf Techn* 64(1): 309-312.
10. Xiao G J, Huang Y. (2015) Constant-load adaptive belt polishing of the weak-rigidity blisk blade. *Int J Adv Manuf Tech* 78(9-12): 1473-1484.
11. He W, Lei M, Bin H Z (2009) Iso-parametric CNC tool path optimization based on adaptive grid generation. *Int J Adv Manuf Tech* 41(5): 538-548.

12. Pan Z X, Polden J, Larkin N, Stephen V D, Norrish J (2012) Recent progress on program-ming methods for industrial robots. *Robotics and Computer-Integrated Manufacturing*, 28(2): 87–94.
13. Feng H, Teng Z J (2005) Iso-planar piecewise linear NC tool path generation from discrete measured data points. *Comput Aided Design* 37(1): 55-64.
14. Kiswanto, G.; Lauwers, B.; Kruth, J.P. (2007) Gouging elimination through tool lifting in tool path 104 generation for five-axis milling based on faceted models. *The International Journal of Advanced Manufacturing Technology*, 32(3): 293-309.
15. Balabokhin A, Tarbutton J (2017) “Iso-scallop tool path building algorithm ‘based on tool performance metric’ for generalized cutter and arbitrary milling zones in 3-axis CNC milling of free-form triangular meshed surfaces.” *J Manuf Process* 28(3): 565-572.
16. Su C, Jiang X, Huo G Y (2020) “Initial tool path selection of the iso-scallop method based on offset similarity analysis for global preferred feed directions matching.” *Int J Adv Manuf Tech* 106(7): 2675-2687.
17. Sun Y W, Guo D M, Jia Z Y (2006) “Iso-parametric tool path generation from triangular meshes for free-form surface machining.” *Int J Adv Manuf Tech* 28(7-8): 721-726.
18. Elber G, Cohen E (1994) “Toolpath generation for freeform surface models.” *Comput Aided Design* 26(6): 490-496.
19. Can A, Ünüvar A (2010) “A novel iso-scallop tool-path generation for efficient five-axis machining of free-form surfaces.” *Int J Adv Manuf Tech* 51(9-12): 1083-1098.
20. Senatore J, Monies F, Redonnet J M (2005) “Analysis of improved positioning in five-axis ruled surface milling using envelope surface.” *Comput Aided Design* 37(10): 989-998.

21. Ding S, Mannan M A, Poo A N (2003) “Adaptive iso-planar tool path generation for machining of free-form surfaces.” *Comput Aided Design* 35(2): 141-153.